



# NMR characterization of H<sub>2</sub>O<sub>2</sub> hydrogen exchange

Tayeb Kakeshpour, Ad Bax\*

Laboratory of Chemical Physics, National Institute of Diabetes and Digestive and Kidney Diseases, Bethesda, MD 20892, USA



## ARTICLE INFO

### Article history:

Received 21 September 2021

Revised 14 October 2021

Accepted 16 October 2021

Available online 19 October 2021

### Keywords:

CEST

Hydrogen peroxide

Biological fluid

Hydrogen exchange

sensitivity-enhanced NMR

pH dependence

## ABSTRACT

Quantification of H<sub>2</sub>O<sub>2</sub> concentration in aqueous solutions is of interest in many fields. It usually is based on indirect methods that rely on oxidation reactions that turn on/off fluorescent probes. Such methods can suffer from reaction incompleteness and interfering chemical species. We describe optimization of NMR detection that enables direct quantification of H<sub>2</sub>O<sub>2</sub> down to the nanomolar range. Taking advantage of fast hydrogen exchange (HX) between H<sub>2</sub>O<sub>2</sub> and water permits the use of very short interscan delays, greatly increasing sensitivity. The specific acid-, base- and water-catalyzed HX rates at 2 °C were measured to be  $2.1 \times 10^7$ ,  $6.1 \times 10^9$ , and  $1.4 \times 10^{-1} \text{ M}^{-1}\text{s}^{-1}$ , respectively, which result in a minimum HX rate at pH 6.2. Furthermore, the exchange is accelerated by general acid/base catalysis. MES and phosphate buffers catalyze HX strongest in their unprotonated forms. For imidazole, only the unprotonated form catalyzes HX, which contrasts with acetic acid where only the protonated state catalyzes exchange. Inorganic salts such as sodium chloride and azide have negligible effect on HX. We present optimal conditions for accurate measurement of H<sub>2</sub>O<sub>2</sub> concentrations as low as 40 nM in aqueous samples in a few hours.

Published by Elsevier Inc.

## 1. Introduction

Hydrogen peroxide (H<sub>2</sub>O<sub>2</sub>) is found in biological systems [1,2] as well as ambient air, rain and the upper atmosphere [3]. H<sub>2</sub>O<sub>2</sub> in respiratory fluids has been reported [4] and may be implicated in the chemical degradation of airborne virus, which is known to occur faster at a relative humidity where the respiratory droplet does not fully dehydrate [5]. Thus, reliable and accurate quantification of H<sub>2</sub>O<sub>2</sub> is important in many areas, ranging from atmospheric science to respiratory viral disease. Recent work has shown that H<sub>2</sub>O<sub>2</sub> forms spontaneously when water condenses to form microdroplets [6]. In related work it was shown that H<sub>2</sub>O<sub>2</sub> generation associated with ultrasonic cavitation of water, used in commercial humidifiers, varies strongly with atmospheric humidity, a finding with potentially important implications for the duration airborne respiratory virus remains viable [7].

H<sub>2</sub>O<sub>2</sub> is commonly quantified via indirect methods that rely on its chemical reaction with fluorogenic probes that increase in quantum yield upon oxidation [8]. Consequently, these methods are susceptible to chemical interference in complex biological samples, as well as reaction incompleteness resulting from the slow kinetics of catalyst-free H<sub>2</sub>O<sub>2</sub> oxidations. For example, the conversion of aryl boronate compounds to fluorescent phenolic derivatives upon oxidation by H<sub>2</sub>O<sub>2</sub> is the most utilized reaction among

the indirect methods. However, this reaction is sluggish (typical rate of  $1\text{--}2 \text{ M}^{-1}\text{s}^{-1}$ ) [9,10] and considerably slower than that of other interfering reactive species such as ONOO<sup>-</sup> ( $10^6 \text{ M}^{-1}\text{s}^{-1}$ ) and HOCl ( $10^4 \text{ M}^{-1}\text{s}^{-1}$ ), thus posing a problem in quantitative analysis [11].

Here, we demonstrate that by optimization of experimental parameters, direct NMR detection of H<sub>2</sub>O<sub>2</sub> in water is readily possible down to the nanomolar range, thereby providing direct quantitative information on its concentration. In water, the NMR spectrum of H<sub>2</sub>O<sub>2</sub> features an exchange-broadened line with a unique chemical shift of around 11 ppm, that previously has been used for H<sub>2</sub>O<sub>2</sub> quantification down to a concentration of 1 mM [12]. Subsequently, Tsiafoulis and Gerothanassis showed that 6-fold dilution of aqueous H<sub>2</sub>O<sub>2</sub> into dimethyl sulfoxide slows down hydrogen exchange (HX) and allows cooling the sample to  $-13 \text{ }^\circ\text{C}$ , thereby sharpening the resonance and achieving a detection limit as low as 20 μM (corresponding to 120 μM in the original aqueous solution) [13]. This method has been used for quantification of H<sub>2</sub>O<sub>2</sub> in plant extracts [14] and cosmetic products [15]. More recently, Ryoo *et al.* exploited the chemical exchange saturation transfer (CEST) technique in combination with the ultrafast Z-spectroscopic method for highly sensitive detection of H<sub>2</sub>O<sub>2</sub> in aqueous solutions, and demonstrated detection in the low millimolar range in as little as 2 s [16]. This method takes advantage of the rapid HX between H<sub>2</sub>O<sub>2</sub> and H<sub>2</sub>O protons and measures the effect of saturating the weak H<sub>2</sub>O<sub>2</sub> resonance on the intense

\* Corresponding author.

H<sub>2</sub>O signal, but quantitative analysis requires accurate knowledge of the H<sub>2</sub>O<sub>2</sub> HX rate. In related work, Buljubasich *et al.* measured the effect of H<sub>2</sub>O<sub>2</sub> on the water transverse relaxation rate as a function of pH and concentration [17]. In an elegant application, they then used the extracted parameters to follow the kinetics of heterogeneously catalyzed H<sub>2</sub>O<sub>2</sub> decomposition [18].

In contrast to previous efforts that relied on organic co-solvents to slow the HX rate and thereby sharpen the H<sub>2</sub>O<sub>2</sub> resonance, our approach to measuring H<sub>2</sub>O<sub>2</sub> takes advantage of the rapid exchange of H<sub>2</sub>O<sub>2</sub> protons with water, similar to CEST [19]. Combined with selective excitation of the downfield region of the spectrum, which leaves the water magnetization unperturbed, the H<sub>2</sub>O<sub>2</sub> *z* magnetization then returns to its Boltzmann equilibrium value at the rate of HX, which is much faster than its longitudinal relaxation rate. This rapid recovery of *z* magnetization permits the use of short interscan delays, only limited by the time needed to collect the free induction decay.

Here, we evaluate some of the most important factors that impact HX rates, including pH, temperature, and buffer concentration. Anbar *et al.* have previously studied the pH dependence of the H<sub>2</sub>O<sub>2</sub> HX rate [20]. However, their measurements applied to the molar concentration regime and their pH of minimum HX rate differs substantially from our results at dilute concentrations. We also investigate the effect of common pH buffers, some of which share functional groups with amino acid sidechains and are shown to catalyze HX. Furthermore, we evaluate the effect of NaCl, which is usually present in biological fluids at high concentration.

## 2. Experimental section

### 2.1. NMR sample preparation

In a typical sample, MES stock buffer solution (10  $\mu$ L, 50 mM in D<sub>2</sub>O) was added to the analyte (490  $\mu$ L) followed by adjusting the pH to within  $\pm 0.05$  pH units of the desired value using a glass electrode. Regular 5 mm NMR tubes and a 600 MHz Avance III Bruker NMR spectrometer equipped with a non-cryogenic probe were used for all measurements unless otherwise mentioned.

### 2.2. Commercial H<sub>2</sub>O<sub>2</sub> standardization

The concentration of our commercial source of H<sub>2</sub>O<sub>2</sub> (30% w/w; Fiscer Scientific) was validated from the relative intensities of the H<sub>2</sub>O<sub>2</sub> and H<sub>2</sub>O resonances, observed following a small flip angle pulse.

### 2.3. *R*<sub>1</sub> measurement

Inversion recovery *T*<sub>1</sub> measurements were carried out with the standard Bruker pulse sequence but replacing the non-selective 180° and 90° pulses by Gaussian shaped pulses of 3.5 ms duration. Variable recovery delays of 0.1, 2, 5, 10, 15, 20, 30, 50 and 120 ms were used. H<sub>2</sub>O<sub>2</sub> intensities were fitted to  $I(t)/I_0 = 1 - A_1 \exp(-R_1 t)$ , in which the fitted parameters, *A*<sub>1</sub> and *R*<sub>1</sub>, are the preexponential factor and longitudinal relaxation rate, respectively; *I*(*t*) represents the spectral intensity for a recovery delay of duration *t*; and *I*<sub>0</sub> corresponds to the intensity obtained in the absence of the 180° pulse. Interscan delays of 300 ms were used.

### 2.4. *R*<sub>2</sub> measurements

An interleaved Hahn echo experiment was used for H<sub>2</sub>O<sub>2</sub> transverse relaxation rate measurements, with the non-selective 90° and 180° pulses replaced by Gaussian shaped pulses of 3.5 ms duration, and using Hahn echo delay durations of 0.1, 2, 5, 10,

15, 20, 30, 50 and 120 ms. A standard EXORCYCLE phase cycling scheme [21] was used to remove the effect of 180° pulse imperfections. The data were fitted to  $I(t) = A_2 \exp(-R_2 t)$ , in which the fitted parameters, *A*<sub>2</sub> and *R*<sub>2</sub>, are the preexponential factor and the transverse relaxation rate, respectively. Interscan delays of 300 ms were used.

### 2.5. HX rate measurement

Considering that *R*<sub>1</sub>  $\approx$  *R*<sub>2</sub> and that both rates are multiple orders of magnitude larger than the natural *R*<sub>1</sub> and *R*<sub>2</sub> rates for pure water (assumed to be comparable to pure H<sub>2</sub>O<sub>2</sub>), measured *R*<sub>1</sub> and *R*<sub>2</sub> rates are effectively equivalent to HX rates. Therefore, the Hahn echo *R*<sub>2</sub> experiment was used for measuring HX rates, neglecting the very small contribution of natural transverse relaxation. Typically, Hahn echo delay durations of 0.1, 2, 5, 10, 15, 20, 30, 50 and 120 ms were used but for fast exchanging samples, durations of 0.1, 0.3, 2, 3, 5, 7, 10, 17 and 60 ms were used.

## 3. Results and discussion

At room temperature, a 1 mM H<sub>2</sub>O<sub>2</sub> sample in pure water, containing 2% D<sub>2</sub>O, yields a weak exchange-broadened resonance at 11.3 ppm and a 55,000 times stronger water signal at the center of the spectrum, consistent with previous reports [12]. This large dynamic range adversely impacts the sensitivity attainable for the H<sub>2</sub>O<sub>2</sub> signal. Due to fast exchange of H<sub>2</sub>O<sub>2</sub> protons with those of H<sub>2</sub>O, presaturation of the water signal obliterates the H<sub>2</sub>O<sub>2</sub> signal and selective excitation with a shaped pulse, centered at 11.3 ppm, is used instead.

As previously reported [13], the HX rate is strongly temperature dependent and the H<sub>2</sub>O<sub>2</sub> resonance narrows considerably upon cooling the sample to 2 °C (Fig. 1). Therefore, this temperature is used for all subsequent measurements.

Upon addition of 50 mM phosphate buffer, used to evaluate the pH dependence of the H<sub>2</sub>O<sub>2</sub> resonance line width, we observed that phosphate strongly broadens the H<sub>2</sub>O<sub>2</sub> resonance across acidic, neutral and basic pH values, making it difficult to detect and indicating that phosphate catalyzes HX. For comparison, a sample containing only 1 mM of 2-(*N*-morpholino) ethanesulfonic acid (MES) buffer showed a fairly sharp resonance with a line width of *ca* 15

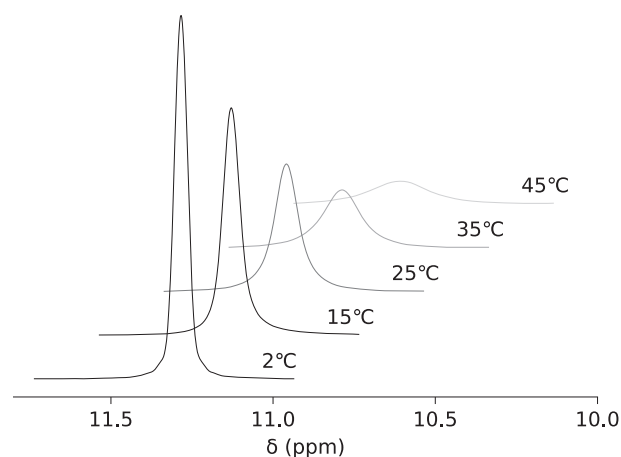


**Fig. 1.** NMR spectra of 1 mM H<sub>2</sub>O<sub>2</sub> in water, highlighting the temperature-dependent HX-related broadening of the signal. The sample contains 2% D<sub>2</sub>O and spectra were recorded at 600 MHz using a non-cryogenic probe, with 256 scans for a total measurement time of *ca* 15 s. The signal resulted from excitation with a 3.2-ms Gaussian shaped 90° excitation pulse, centered at the H<sub>2</sub>O<sub>2</sub> resonance. The chemical shift scale is referenced to internal (CH<sub>3</sub>)<sub>3</sub>SiCH<sub>2</sub>CH<sub>2</sub>CH<sub>2</sub>SO<sub>3</sub>Na (DSS).

Hz in the 5.5–6.0 pH range, consistent with results of Ryoo *et al.* [16].

To further investigate HX, we used H<sub>2</sub>O<sub>2</sub>-selective pulses to measure the selective longitudinal and transverse relaxation rates,  $R_1$  and  $R_2$  (Fig. 2). At pH 5.9, measured  $R_1$  and  $R_2$  rates were the same within error of the measurement ( $45.0 \pm 0.4$  vs.  $45.3 \pm 0.4$  s<sup>-1</sup>, respectively). This result indicates that the loss of longitudinal and transverse magnetization is dominated by the exchange of H<sub>2</sub>O<sub>2</sub> hydrogens with water. Thus, to a good approximation, the  $R_1$  and  $R_2$  measurements correspond to the HX rate. As shown in Fig. 2, the excited H<sub>2</sub>O<sub>2</sub> magnetization decays to *ca* 10% of its initial value in as little as 50 ms, defining this duration as close to the approximate optimal acquisition time for recording spectra with adequate sensitivity and resolution. Together with a short interscan delay of 1 ms, this allows for recording *ca* 18 scans per second, thereby increasing the signal to noise ratio per unit of time compared to recording other small molecule NMR spectra.

A plot of the HX rates, derived from an interleaved Hahn echo experiment, against pH shows a well-defined minimum at pH 6.2 (Fig. 3). The plot is similar to those of peptide backbone amides except that the latter have a minimum near pH 4 [22]. Similar to proteins [23,24], the first order apparent exchange rate ( $k_{ex}$ ) can be written as

$$k_{ex} = k_{H_2O}[H_2O] + k_{MES}[MES] + k_H \times 10^{-pH} + k_{OH} \times 10^{-pOH} \quad (1)$$

in which  $k_{H_2O}$ ,  $k_{MES}$ ,  $k_H$  and  $k_{OH}$  are water, MES, acid and base catalyzed rate constants, respectively, and pH and pOH are the negative of the base 10 logarithm of the H<sup>+</sup> and OH<sup>-</sup> ion concentrations, respectively. Fitting the data to eq. (1) (dashed line in Fig. 3) yields values of  $12 \pm 1$  s<sup>-1</sup> for  $k_{H_2O}[H_2O] + k_{MES}[MES]$ ;  $k_H = (2.1 \pm 0.1) \times 10^7$  M<sup>-1</sup>s<sup>-1</sup> and  $k_{OH} = (6.1 \pm 0.2) \times 10^9$  M<sup>-1</sup>s<sup>-1</sup>. The change of pH upon cooling of the sample from 20 to 2 °C was determined by linear extrapolation of glass electrode measurements at 20 and 5 °C [25]. For calculating pOH at 2 °C, a water dissociation constant of  $pK_w = 14.86$  was used [26]. By varying the MES buffer concentration while keeping the sample at pH 6.2 and 2 °C,  $k_{MES}$  and subsequently  $k_{H_2O}$  were extracted (Fig. 4; Table 1).

The contribution of the unprotonated and protonated MES species to the exchange catalysis was dissected by varying the pH. Upon increasing the pH from 5.6 to 6.8 (at 2 °C), the mole fraction of the unprotonated MES increases from 0.14 to 0.71 (calculated using MES ionization enthalpy of +3.54 kcal/mol for pKa temperature correction). This pH increase resulted in an increase in the

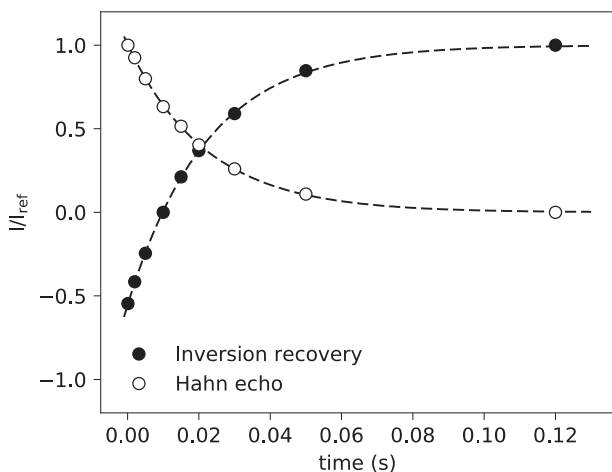


Fig. 2.  $R_1$  and  $R_2$  measurements of the H<sub>2</sub>O<sub>2</sub> signal at 11.3 ppm on a sample at 2 °C containing 1 mM H<sub>2</sub>O<sub>2</sub> buffered at pH 5.9 using 1 mM MES.

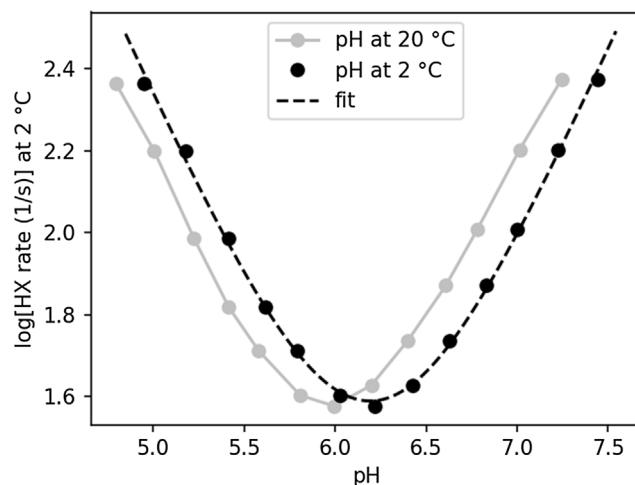


Fig. 3. The pH dependence of the HX rate of H<sub>2</sub>O<sub>2</sub> protons with water. The pH of the samples was adjusted at 20 °C and the rates were measured at 2 °C. Samples contain 1 mM MES and 1 mM H<sub>2</sub>O<sub>2</sub>. The dashed line represents the best fit to equation (1).

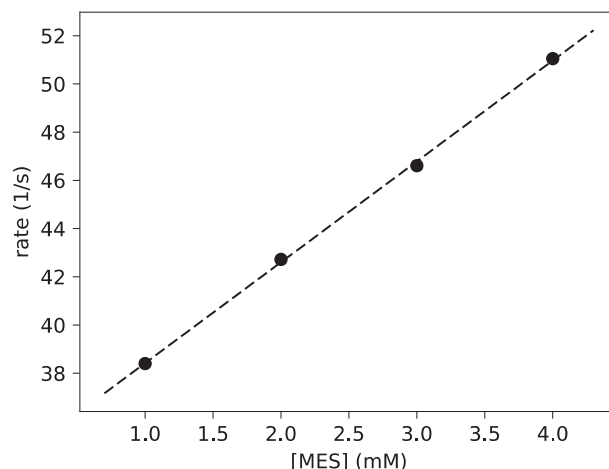


Fig. 4. Dependence of the H<sub>2</sub>O<sub>2</sub> HX rate on the MES concentration at pH 6.2, 2 °C.

slope of the HX rates *versus* MES concentration (Fig. 5A), indicating that the unprotonated form of MES catalyzes the exchange more than its protonated counterpart. The MES contribution to the exchange rate from the protonated and unprotonated forms can be written as

$$k_{ex,MES} = C + (k_a X_a + k_b X_b)[MES] \quad (2)$$

in which  $k_a$  and  $k_b$  are the general acid- and base-catalyzed rate constants, respectively, and  $X_a$  and  $X_b$  denote the corresponding mole fractions. The term  $C$  is a constant accounting for water as well as specific acid- and base-catalyzed contributions, which vary with pH. By minimizing the residuals function,

Table 1  
Acid, base, water, and MES HX rate constants at 2 °C.

Catalyst	$k_{ex}$ (M <sup>-1</sup> s <sup>-1</sup> )
H <sub>3</sub> O <sup>+</sup>	$(2.1 \pm 0.1) \times 10^7$
OH <sup>-</sup>	$(6.1 \pm 0.2) \times 10^9$
H <sub>2</sub> O	$(1.4 \pm 0.4) \times 10^{-1}$
MES <sup>pH 6.2</sup>	$(4.2 \pm 0.1) \times 10^3$

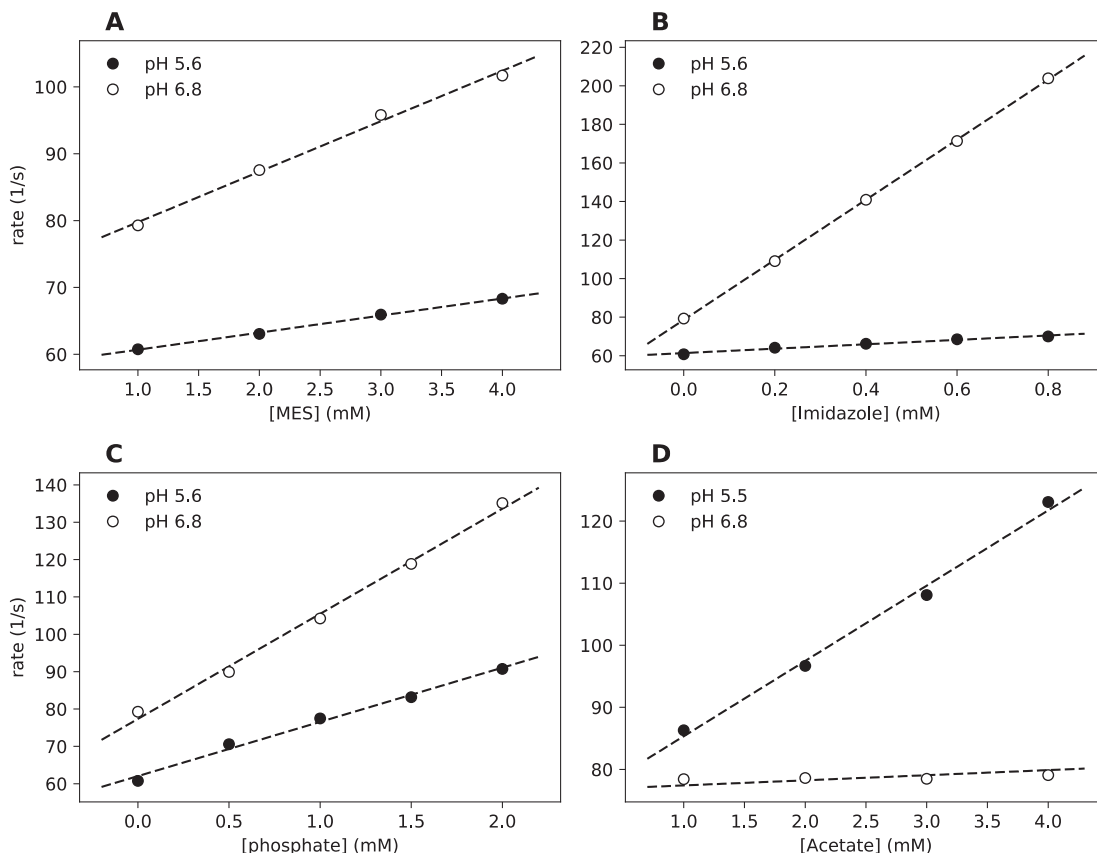


**Fig. 5.** Concentration dependence of H<sub>2</sub>O<sub>2</sub> HX rates for (A) MES (B) imidazole (C) phosphate and (D) acetate at two pH values, 2 °C.

$$\chi^2 = \sum_i \{k_{ex}^{obs(i)} - (C_i + (k_a X_a^i + k_b X_b^i)[MES])\}^2 \quad (3)$$

$k_a$  and  $k_b$  values can then be obtained, where  $i$  runs over all the experimental pH values, and the mole fractions at each pH are calculated using the literature buffer pK<sub>a</sub> values and their temperature dependence [25]. The unprotonated form of MES is found to catalyze the exchange about eight times stronger than its protonated form (Table 2), presumably resulting from the involvement of the MES tertiary amine in the HX catalysis. Similarly, the free nitrogen of the unprotonated imidazole buffer catalyzes exchange nearly 100-fold stronger than MES, while its protonated form has no detectable effect on HX. Analogous to the above cases, the more basic phosphate species, HPO<sub>4</sub><sup>2-</sup>, catalyzes HX about five-fold more than H<sub>2</sub>PO<sub>4</sub><sup>-</sup>. In contrast, acetic acid catalyzes the exchange slope of the line at pH 5.5 compared to pH 6.8 (Fig. 4D). Monovalent inorganic salts have only small effects on the exchange: Addition of 50 mM sodium chloride or azide increases the HX rates from  $38.1 \pm 0.3 \text{ M}^{-1} \text{ s}^{-1}$ , in the absence of salt, to  $44.8 \pm 0.7 \text{ M}^{-1} \text{ s}^{-1}$  and  $58.9 \pm 0.2 \text{ M}^{-1} \text{ s}^{-1}$ , respectively (Fig. 6).

**Table 2**

Contribution of protonated and unprotonated forms of several buffers and salts to the H<sub>2</sub>O<sub>2</sub> HX rate.

Compound	$k_{ex} (\text{M}^{-1}\text{s}^{-1})$	
	protonated	unprotonated
MES	$(1.3 \pm 0.4) \times 10^3$	$(1.0 \pm 0.1) \times 10^4$
Imidazole	$<10^3$	$(8.0 \pm 0.1) \times 10^5$
Phosphate	$(1.3 \pm 0.1) \times 10^4$	$(6.6 \pm 0.5) \times 10^4$
Acetic acid	$(8.7 \pm 0.4) \times 10^4$	$<10^2$
NaCl	-	$(1.3 \pm 0.2) \times 10^2$
NaN <sub>3</sub>	-	$(4.2 \pm 0.1) \times 10^2$

To test the sensitivity of the NMR detection method, a 40 nM H<sub>2</sub>O<sub>2</sub> sample was prepared with the spectrum recorded on a 600 MHz instrument equipped with a Bruker TCI cryoprobe (Fig. 7). A signal to noise (S/N) of 3.8 was achieved after 100 K scans (97 min). This S/N corresponds to an error of only ~ 25% in the quantification of a 40-nM H<sub>2</sub>O<sub>2</sub> sample and a detection limit of 32 nM. Based on typical concentrations reported in the literature [2,3,15], this sensitivity suffices for many applications, including quantification of H<sub>2</sub>O<sub>2</sub> in exhaled breath condensate, air, rain, blood and other biological fluids.

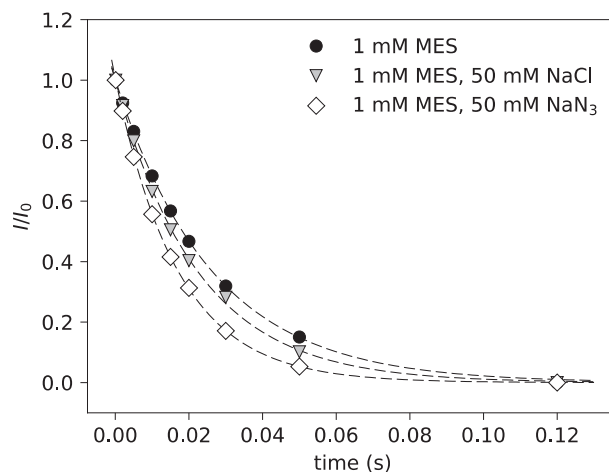


**Fig. 6.** Measurement of HX rates for samples containing 50 mM NaCl and NaN<sub>3</sub> compared with rates of the salt-free sample (1 mM MES).

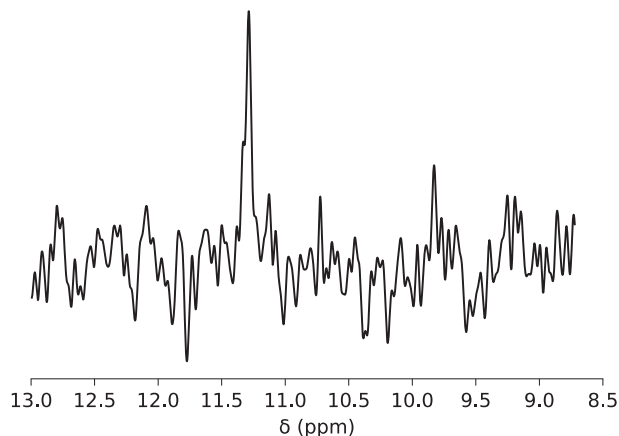


**Fig. 7.** NMR spectrum of a 40-nM  $\text{H}_2\text{O}_2$  sample in water containing 2%  $\text{D}_2\text{O}$  and 1 mM MES. The pH was adjusted to 6.0 at 20 °C, and the spectrum was obtained at 2 °C using a 600-MHz Bruker NEO spectrometer equipped with a TCI cryoprobe. To further reduce excitation of the water resonance for this very dilute sample, selectivity of the excitation pulse was increased by extending the duration of the Gaussian shaped excitation pulse to 6 ms. An acquisition time of 50 ms and an interscan delay of 1 ms, with 102,400 scans for a total measurement time of *ca* 1.6 h were used.

#### 4. Conclusions

In the absence of pH-dependent HX catalysts, at dilute  $\text{H}_2\text{O}_2$  concentrations the narrowest resonance is obtained at pH values of 6.0 at 20 °C (or 6.2 at 2 °C). The strong temperature dependence of the HX rate results in narrowing of the resonance when cooling samples to just above the freezing point of water. Unlike peptide backbone amides, water-catalyzed HX of  $\text{H}_2\text{O}_2$  is significant near the pH value where the combined acid- and base-catalyzed HX is at a minimum. Our measurements show that while phosphate species and common functional groups in proteins such as imidazole rings and carboxylic acids can catalyze HX, sodium chloride or azide do not affect the exchange significantly. The present characterization of the  $\text{H}_2\text{O}_2$  HX rates serves as the basis for preparing the sample conditions needed for quantifying the presence of small quantities of  $\text{H}_2\text{O}_2$  in a wide range of biological fluids and other aqueous samples. Taking advantage of the rapid HX of water, selective excitation of the  $\text{H}_2\text{O}_2$  resonance permits the use of short delays between scans, yielding a sensitivity on a 600 MHz instrument equipped with a triple resonance cryogenic probe of *ca* 25:1 per 6 min for a 1- $\mu\text{M}$  sample. Single-channel cryogenic probeheads, optimized solely for  $^1\text{H}$  detection, could further improve the sensitivity of  $\text{H}_2\text{O}_2$  detection by NMR.

#### Declaration of Competing Interest

The authors declare that they have no known competing financial interests or personal relationships that could have appeared to influence the work reported in this paper.

#### Acknowledgements

The authors thank James Baber and Jinfa Ying for technical support and Richard N. Zare and Dennis A. Torchia for helpful discus-

sions. This work was supported by the Intramural Research Program of the National Institute of Diabetes and Digestive and Kidney Diseases.

#### References

- [1] J.R. Stone, S.P. Yang, Hydrogen peroxide: A signaling messenger, *Antioxid. Redox Signaling* 8 (3–4) (2006) 243–270.
- [2] H.J. Forman, A. Bernardo, K.J.A. Davies, What is the concentration of hydrogen peroxide in blood and plasma?, *Arch Biochem. Biophys.* 603 (2016) 48–53.
- [3] H. Sakugawa, I.R. Kaplan, W.T. Tsai, Y. Cohen, Atmospheric hydrogen peroxide, *Environ. Sci. Technol.* 24 (10) (1990) 1452–1462.
- [4] S. Peters, A. Kronseder, S. Karrasch, P.A. Neff, M. Haaks, A.R. Koczulla, P. Reinhold, D. Nowak, R.A. Jörres, Hydrogen peroxide in exhaled air: a source of error, a paradox and its resolution, *ERJ Open Res.* 2 (2) (2016) 00052–2015.
- [5] M.K. Ijaz, A.H. Brunner, S.A. Sattar, R.C. Nair, C.M. Johnsonlussenburg, Survival characteristics of airborne human coronavirus-229E, *J. Gen. Virol.* 66 (1985) 2743–2748.
- [6] J.K. Lee, H.S. Han, S. Chaikasetin, D.P. Marron, R.M. Waymouth, F.B. Prinz, R.N. Zare, Condensing water vapor to droplets generates hydrogen peroxide, *Proc. Natl. Acad. Sci.* 117 (49) (2020) 30934–30941.
- [7] M.T. Dulay, C.A. Huerta-Aguilar, C.F. Chamberlayne, R.N. Zare, A. Davidse, S. Vukovic, Effect of relative humidity on hydrogen peroxide production in water droplets, *QRB Discovery* 2 (2021) e8.
- [8] F. Rezende, R.P. Brandes, K. Schroder, Detection of Hydrogen Peroxide with Fluorescent Dyes, *Antioxid. Redox Signaling* 29 (6) (2018) 585–602.
- [9] H.G. Kuivila, Electrophilic Displacement Reactions. III. Kinetics of the Reaction between Hydrogen Peroxide and Benzeneboronic Acid1, *J. Am. Chem. Soc.* 76 (3) (1954) 870–874.
- [10] H.G. Kuivila, A.G. Armour, Electrophilic Displacement Reactions. IX. Effects of Substituents on Rates of Reactions between Hydrogen Peroxide and Benzeneboronic Acid1-3, *J. Am. Chem. Soc.* 79 (21) (1957) 5659–5662.
- [11] J. Zielonka, A. Sikora, M. Hardy, J. Joseph, B.P. Dranka, B. Kalyanaraman, Boronate Probes as Diagnostic Tools for Real Time Monitoring of Peroxynitrite and Hydroperoxides, *Chem. Res. Toxicol.* 25 (9) (2012) 1793–1799.
- [12] N.A. Stephenson, A.T. Bell, Quantitative analysis of hydrogen peroxide by  $^1\text{H}$  NMR spectroscopy, *Anal. Bioanal. Chem.* 381 (6) (2005) 1289–1293.
- [13] C.G. Tsiafoulis, I.P. Gerathanassis, A novel NMR method for the determination and monitoring of evolution of hydrogen peroxide in aqueous solutions, *Anal. Bioanal. Chem.* 406 (14) (2014) 3371–3375.
- [14] P. Charisiadis, C.G. Tsiafoulis, V. Exarchou, A.G. Tzakos, I.P. Gerathanassis, Rapid and Direct Low Micromolar NMR Method for the Simultaneous Detection of Hydrogen Peroxide and Phenolics in Plant Extracts, *J. Agric. Food Chem.* 60 (18) (2012) 4508–4513.
- [15] Y.B. Monakhova, B.W.K. Diehl, Rapid  $^1\text{H}$  NMR determination of hydrogen peroxide in cosmetic products and chemical reagents, *Anal. Methods* 8 (23) (2016) 4632–4639.
- [16] D. Ryou, X. Xu, Y. Li, J.A. Tang, J. Zhang, P.C.M. van Zijl, G. Liu, Detection and Quantification of Hydrogen Peroxide in Aqueous Solutions Using Chemical Exchange Saturation Transfer, *Anal. Chem.* 89 (14) (2017) 7758–7764.
- [17] L. Buljubasich, B. Blümich, S. Stapf, Quantification of  $\text{H}_2\text{O}_2$  concentrations in aqueous solutions by means of combined NMR and pH measurements, *Phys. Chem. Chem. Phys.* 12 (40) (2010) 13166–13173.
- [18] L. Buljubasich, B. Blümich, S. Stapf, Reaction monitoring of hydrogen peroxide decomposition by NMR relaxometry, *Chem. Eng. Sci.* 65 (4) (2010) 1394–1399.
- [19] K.M. Ward, A.H. Aletras, R.S. Balaban, A new class of contrast agents for MRI based on proton chemical exchange dependent saturation transfer (CEST), *J. Magn. Reson.* 143 (1) (2000) 79–87.
- [20] M. Anbar, A. Loewenstein, S. Meiboom, Kinetics of Hydrogen Exchange between Hydrogen Peroxide and Water Studied by Proton Magnetic Resonance 1,2, *J. Am. Chem. Soc.* 80 (11) (1958) 2630–2634.
- [21] G. Bodenhausen, R. Freeman, D.L. Turner, Suppression of artifacts in 2-dimensional J spectroscopy, *J. Magn. Reson.* 27 (3) (1977) 511–514.
- [22] R.S. Molday, S.W. Englander, R.G. Kallen, Primary structure effects on peptide group hydrogen exchange, *Biochemistry* 11 (2) (1972) 150–158.
- [23] S.W. Englander, Hydrogen Exchange and Mass Spectrometry: A Historical Perspective, *J. Am. Soc. Mass Spectrom.* 17 (11) (2006) 1481–1489.
- [24] Y. Bai, J.S. Milne, L. Mayne, S.W. Englander, Primary structure effects on peptide group hydrogen exchange, *Proteins: Struct., Funct., Bioinf.* 17 (1) (1993) 75–86.
- [25] R.N. Goldberg, N. Kishore, R.M. Lennen, Thermodynamic Quantities for the Ionization Reactions of Buffers, *J. Phys. Chem. Ref. Data* 31 (2) (2002) 231–370.
- [26] A.V. Bandura, S.N. Lvov, The Ionization Constant of Water over Wide Ranges of Temperature and Density, *J. Phys. Chem. Ref. Data* 35 (1) (2005) 15–30.